Available online at www.sciencedirect.com

ScienceDirect

Journal homepage: www.elsevier.com/locate/cortex

Clinical Neuroanatomy

Lesion-symptom mapping of language impairments in patients suffering from left perisylvian gliomas

Lucius S. Fekonja [a,b,1,*], *Ziqian Wang* [a,1], *Lea Doppelbauer* [c], *Peter Vajkoczy* [a], *Thomas Picht* [a,b], *Friedemann Pulvermüller* [b,c] and *Felix R. Dreyer* [b,c,d]

[a] *Department of Neurosurgery, Charité - Universitätsmedizin Berlin, Berlin, Germany*
[b] *Cluster of Excellence: "Matters of Activity. Image Space Material", Humboldt University, Berlin, Germany*
[c] *Freie Universität Berlin, Brain Language Laboratory, Department of Philosophy and Humanities, Berlin, Germany*
[d] *Medical School OWL, Bielefeld University, Bielefeld, Germany*

ARTICLE INFO

Article history:
Received 25 January 2021
Reviewed 23 March 2021
Revised 10 May 2021
Accepted 2 August 2021
Action editor Stefano Cappa
Published online 2 September 2021

Keywords:
Glioma
Tumor
White matter
Grey matter
VLSM
Language

ABSTRACT

Brain tumors cause local structural impairments of the cerebral network. Moreover, brain tumors can also affect functional brain networks more distant from the lesion. In this study, we analyzed the impact of glioma WHO grade II-IV tumors on grey and white matter in relation to impaired language function. In a retrospective analysis of 60 patients, 14 aphasic and 46 non-aphasic, voxel-based lesion-symptom mapping (VLSM) was used to identify tumor induced lesions in grey (GM) and white matter (WM) related to patients' performance in subtests of the Aachen Aphasia Test (AAT). Significant clusters were analyzed for atlas-based grey and white matter involvements in relation to different linguistic modalities.

VLSM analysis indicated significant contribution of a posterior perisylvian cluster covering WM and GM to AAT performance averaged across subtests. When considering individual AAT subtests, a substantial overlap between significant clusters for analysis of the token test, picture naming and language comprehension results could be observed.

The WM-cluster intersections reflect the overall importance of the perisylvian area in language function, similarly to GM participations. Especially the constant high percentages of Heschl's gyrus, superior temporal gyrus, inferior longitudinal and middle longitudinal fascicles, but also arcuate and inferior fronto-occipital fascicles highlight the importance of the posterior perisylvian area for language function.

* *Corresponding author*. Charité Universitätsmedizin Berlin, Klinik für Neurochirurgie mit Arbeitsbereich Pädiatrische Neurochirurgie, Campus Charité Mitte, Luisenstraße 64, 10117, Berlin, Germany.
E-mail address: lucius.fekonja@charite.de (L.S. Fekonja).
[1] These authors contributed equally.

https://doi.org/10.1016/j.cortex.2021.08.002

1. Introduction

Brain tumors cause local impairment of the structural cerebral network. Furthermore, brain tumors can also affect functional brain networks located further away from the lesion. In this study, we analyzed the impact of WHO grade II-IV gliomas on gray and white matter in relation to language function.

The investigation of language impairments in glioma patients is of interest both for clinical relevance and for basic science on the neural bases of language. From a clinical perspective it has to be noted that language impairments have a potentially large impact on the quality of life of patients (Hilari & Byng, 2009; Ross & Wertz, 2003). Furthermore, aphasia in glioma patients may directly limit pre-surgical and intra-operative diagnostic methods currently available, namely TMS or DCS based picture naming language mapping. In addition, aphasic disorders possibly diminish the language assessment methods' interpretability (Schwarzer et al., 2018). Thus, from a clinical perspective, it is necessary to relate tumor location and further patient characteristics to language deficits in order to achieve optimal diagnostics, treatment and personalized postoperative therapy tailored to the capabilities and impairments of the individual patients.

From a neuroscientific perspective, the analysis of the relationship between brain lesions and cognitive function in general provides insights into neural substrates underlying these functions. A suitable method to systematically analyze the relationship between lesions and cognitive impairment at group level is voxel-based lesion symptom mapping (Bates et al., 2003). In contrast to fMRI neuroimaging approaches, which provide correlational evidence about the involvement of brain areas in cognitive processing, VLSM and lesion studies allow conclusions on the causal role and necessity of neural substrates for cognitive functions. However, in the scope of linguistic research, VLSM analyses have mainly been performed in patients with vascular diseases such as stroke, which typically lead to large lesions distributed according to the brain's vascular outline. Therefore, it has been argued that there might be a lack of granularity as well as biological biases in lesion loci (Herbet, Lafargue, & Duffau, 2015) and the possibility exists that post-stroke aphasia deficits in part reflect the common blood supply of adjacent and sometimes distant areas, for example that provided by the huge territory of the left middle cerebral artery. Therefore, VLSM analysis of glioma patients may allow conclusions on the neural substrates of language processing with a higher spatial resolution and may thus provide information complementary to inferences drawn from previous VLSMs performed on stroke patients. Here, we used VLSM to relate individual lesion areas with patients' language performance and atlas-based grey and high angular resolution diffusion imaging (HARDI) based white matter involvements with different linguistic modalities as determined by subtests of the Aachen Aphasia Test (AAT) in a retrospective analysis of 60 patients. The included patients were initially considered as fit for awake surgery.

2. Materials & methods

2.1. Ethical standard

The study proposal is in accordance with ethical standards of the Declaration of Helsinki and was approved by the ethics committee of Charité - Universitätsmedizin Berlin (#EA1/016/19). All patients provided written informed consent for medical evaluations and treatments within the scope of the study.

2.2. Patient cohort

We included n = 60 right-handed adult patients (30 females, 30 males, age 53.9 ± 15.6, age range 24–85) in retrospective analysis (Table 1). Only Table 2 patients with initial diagnosis of unilateral glioma WHO grade II-IV tumors in their left hemisphere were included in this study. All patients were native German speakers. Exclusion criteria were recurrent tumors, prior surgical resection or radio- and/or chemotherapy, left-handedness, non-glioma tumors or multicentric tumors and severe naming impairment due to language production deficits which was reflected in the inability to perform the test. The included patients were initially presumed to be eligible for awake surgery.

The lesion overlay covered large parts of the left perisylvian language network, which includes frontal, insular, temporal and parietal lobes (Fig. 1). However, closer inspection shows that the major area of lesion overlap lay in the anterior and middle temporal lobe. Furthermore, the frontal areas were primarily affected by larger lesions, as indicated by Fig. 2, whereas average lesion size intemporal areas was relatively small, thus allowing

Table 1 – Demographics and AAT t-scores.

	Number (%)
Demographics	
Sample size	60
Age (year)	53.92 ± 15.61
Female	30 (50)
Male	30 (50)
Tumor size (cm^3)	44.94 ± 38.48
Glioma degrees (WHO)	
Glioma II	9 (15)
Glioma III	19 (32)
Glioma IV	32 (53)
Tumor locations	
Frontal	16 (27)
Temporal	32 (53)
Insular	6 (10)
Parietal	6 (10)
AAT (T-scores)	
Average	67.02 ± 7.90
Token	68.23 ± 7.42
Naming	66.19 ± 7.16
Repetition	67.53 ± 11.53
Comprehension	66.12 ± 11.47
Reading comprehension	63.97 ± 11.48
Auditory comprehension	64.44 ± 10.43

Values shown are M ± SD or n (%). AAT: Aachen aphasia test.

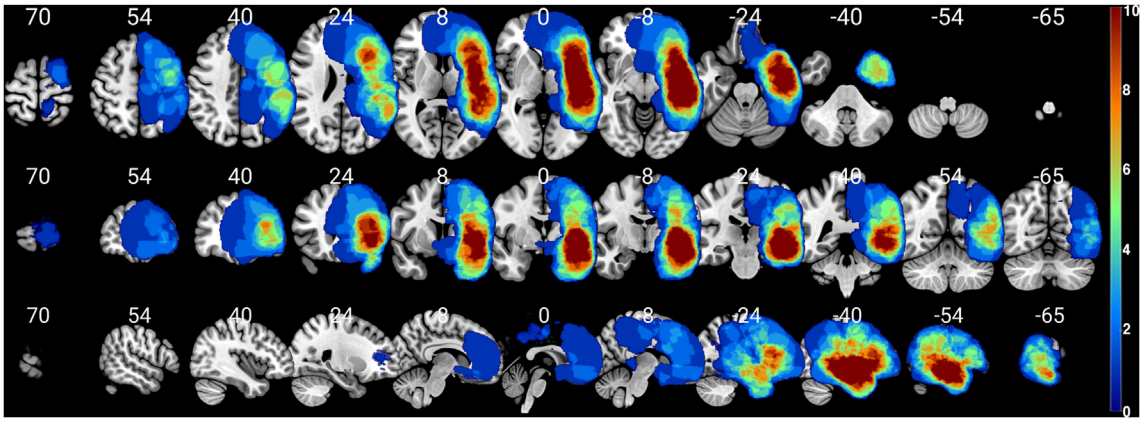

Fig. 1 – Lesion overlay map of all 60 tumor patients. The color bar indicates the number of patients in whom a given voxel was lesioned by a tumor (in range 0–10, warmer colours indicate higher lesion overlay). The numbers above the slices indicate their axial slice positions in Montreal Neurological Institute (MNI) space.

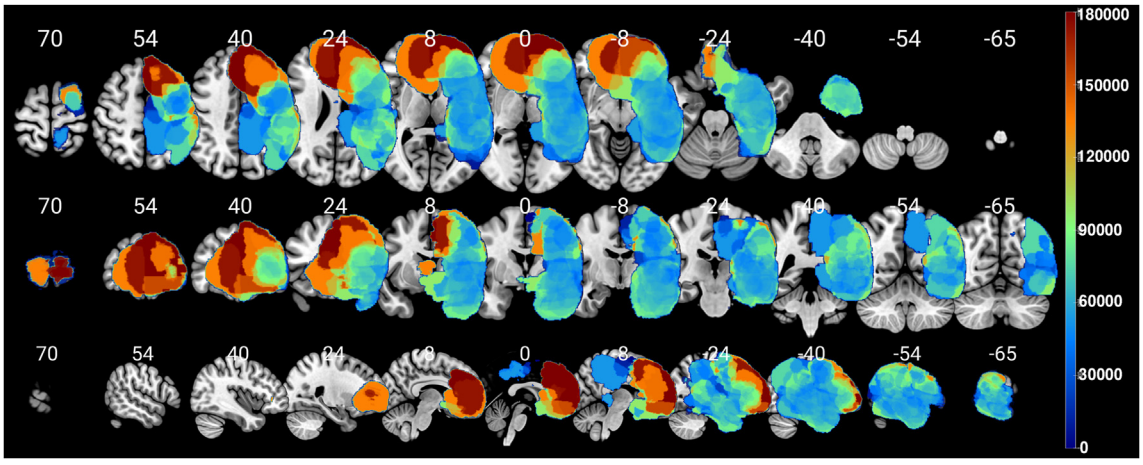

Fig. 2 – Average lesion size per voxel. The color bar indicates the voxel-wise average lesion size (volume in mm^3) of patients with a lesion in a given voxel (in range 0–180,000, warmer colours indicate higher average lesion overlay). The numbers above the slices indicate their axial slice positions in Montreal Neurological Institute (MNI) space.

for fine grained spatial inferences. Handedness was determined using the Edinburgh handedness inventory prior to aphasia assessment (Oldfield, 1971). The inclusion/exclusion criteria were established prior to data analysis.

2.3. *Aphasia assessment*

All patients under investigation underwent the AAT (Huber, Poeck, & Willmes, 1984), a standardized German aphasia test battery, as part of our pre-operative clinical examination. The AAT allows an assessment of spontaneous speech on various neurolinguistically defined levels of observation. Subtests differentiate and objectively assess linguistic impairments in speaking, reading, writing, naming, and comprehension regarding various linguistic units and regularities. Another component is the Token Test, which provides additional information to distinguish aphasia from non-aphasic disorders and to assess the severity of aphasia. We used a subset of test parts, which covered all offered assessment levels, due to clinical time constraints. AAT subtests included in this version were Token Test, Verbal Repetition, Naming and Language Comprehension (of written and auditory language, which also delivers a combined comprehension measure across both modalities). The AAT provides standardized t-scores for psychometric individual case diagnostics which also allow for classification of severity of aphasic symptoms.

2.4. *Imaging*

2.4.1. *MRI acquisition*

MRI data were acquired on a Siemens Skyra 3T scanner (Erlangen, Germany) equipped with a 32-channel receiver head coil at Charité - Universitätsmedizin Berlin, Department of Neuroradiology. These data consisted of a high-resolution contrast enhanced T1c weighted anatomical (TR/TE/TI 2300/2.32/900 m sec, 9° flip angle, 256 × 256 matrix, 1 mm isotropic voxels, 192 slices), for a total acquisition time of 5 min. T2-weighted, 3D fluid attenuated inversion recovery (FLAIR) and subtraction sequences were additionally performed.

2.5. Spatial normalization & lesion masking

To optimize the registration process to Montreal Neurological Institute (MNI) International Consortium for Brain Mapping (ICBM) 152 space, we skull-stripped all T1 images applying the ANTs brain extraction tool in combination with the public ANTs/ANTsRIXI brain template (https://doi.org/10.6084/m9.figshare.915436.v2) prior to MNI space registration (Avants et al., 2011). Additionally, we performed lesion masking with ITK-SNAP using the anatomical T1c, T2 and FLAIR images in standard space (Yushkevich et al., 2006). All patients' images were registered to standard space (MNI ICBM 152 non-linear 6th generation symmetric average brain stereotaxic registration model) using Advanced Normalization Tools (ANTs) with the Symmetric Normalization (SyN) transformation model (Avants et al., 2011; Grabner et al., 2006).

2.6. VLSM

In preparation of VLSM analysis, demographic and tumor characteristics were analyzed for influences on AAT performance (averaged across subscales and separately for individual subscales), to identify relevant covariates for further analyses. To this end the influence of age on AAT measures was investigated using the Pearson correlation coefficient. The performance of male and female patients was compared using a two-sample t-test. Furthermore, WHO tumor gradings were compared using an analysis of variance (ANOVA) with subsequent two-sample post hoc t-test.

To evaluate effects of voxel-wise lesions on language functions, VLSM was applied using the VLSM toolbox (https://aphasialab.org/vlsm/), Version 2.5, with MATLAB (MathWorks, Natick, MA, US), version R2014b (Bates et al., 2003). This analysis compared the AAT results of patients with and without lesions in a given voxel using a general linear model. The lesion size was added as a covariate to this analysis in order to account for a higher spatial specificity of inferences that can be drawn from more focal lesions. In addition, demographic and lesion characteristics of patients were included in analysis as covariates in case these variables were indicated to be related to AAT performance.

The analysis was confined to voxels showing a minimal lesion overlap of n = 5 voxels. Voxel-wise results were thresholded at $p < .05$ and a permutation testing-based family-wise error rate (FWE) corrected $p < .05$ was applied on the cluster-level. The power map of this analysis is presented in Fig. 3, demonstrating sufficient power (1- $\beta > .7$) in inferior, middle and superior temporal cortices, as well as in the insula and inferior frontal areas. Overview lesion focality per voxel in the sample under investigation was created in order to provide a descriptive measure of potential area-specific biases in the spatial resolution of VLSM results (see Fig. 2). This measure was defined as the average lesion size of patients with a lesion in a given voxel.

VLSM was performed on AAT results averaged across scales, as well as on the individual subscales of object naming, verbal repetition and language comprehension. Language comprehension was tested combined and separately for written or auditory comprehension.

2.7. White and grey matter atlases

We used the Illinois Institute of Technology (IIT) Human Brain Atlas (Zhang & Arfanakis, 2018) to compute the intersections of VLSM clusters and white matter (WM) in order to identify involved fiber bundles. The IIT Human Brain Atlas (v.5.0) offers 42 major white matter bundle masks, obtained from artifact free HARDI MRI data of 72 subjects and subsequent RecoBundles tract generation (Garyfallidis et al., 2018). To analyze the intersections of involved fiber bundles, the volumes (mm^3) of each cluster and atlas-based fiber bundle mask were computed with FSL (FMRIB Software Library v6.0, FMRIB Software Library, FMRIB = Oxford Centre for Functional MRI of the Brain) tools (Jenkinson, Beckmann, Behrens, Woolrich, & Smith, 2012). Finally, we generated a five-tissue-type (5TT) segmented tissue image (Smith, Tournier, Calamante, & Connelly, 2012) of the T1 MNI image to obtain probability WM, GM, subcortical GM and CSF masks. The WM mask was binarized (intensity

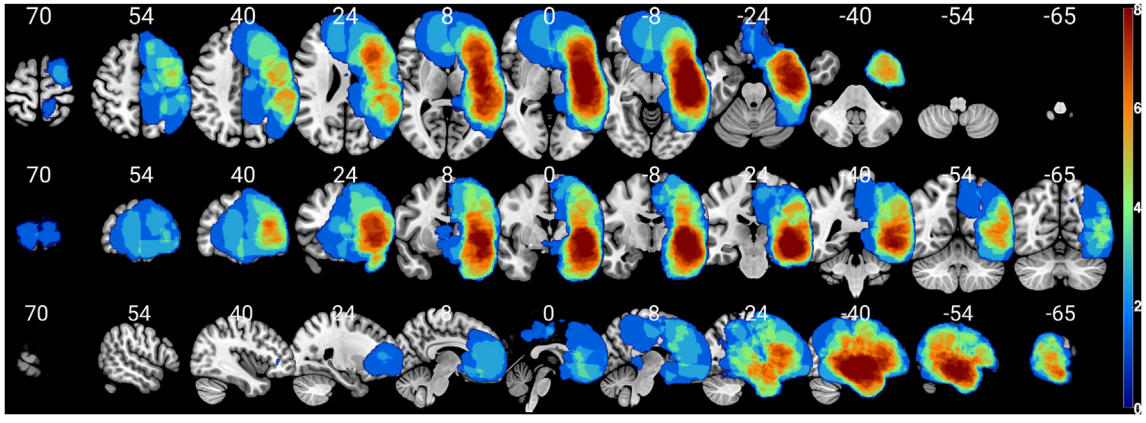

Fig. 3 – VLSM power map with FWE-corrected $p < .05$. The color bar indicates the voxel-wise statistical power for VLSM analysis (blue = low power, red = high power). The numbers indicate the axial slice positions in MNI space.

values > .5 = 0, <.5 = 1) and used to refine the size of IIT WM parcellations and exclude possible grey matter (GM).

In addition to WM-VLSM cluster intersections, we computed GM-VLSM cluster intersections in relation to the Automated Anatomical Labeling (AAL3) atlas (Rolls, Huang, Lin, Feng, & Joliot, 2020) to define cortical regions of interests (ROIs). The AAL3 labelling offers a whole brain parcellation of 170 ROIs. Subsequently, all AAL3 ROIs were computed as volumes (mm^3) using FSL tools, for the computation of WM ROIs (Jenkinson et al., 2012) as described above (see 2.7). Mirroring abovementioned WM parcellation refinement (see 2.7), the 5TT image derived WM mask was binarized (intensity values > .5 = 1, <.5 = 0) and used to refine AAL3 GM parcellations.

Furthermore, we calculated how many patients had a lesion in each GM and WM area and assigned them to binary area-wise affected (1) or non-affected (0) groups. A series of two-sample *t*-test with Bonferroni-Holm correction was used for post-hoc comparisons of all AAT t-scores of above mentioned two groups.

2.8. *Data availability*

The data that support the findings of this study are not publicly available due to information that could compromise the privacy of the research participants but are available from the corresponding author on reasonable request.

3. Results

3.1. AAT

AAT results showed no language impairments in most of the 60 patients included in the analysis (76.7%, n = 46), whereas 11.7% (n = 7) exhibited mild and another 11.7% (n = 7) of patients showed moderate aphasia symptoms.

3.2. *Influence of demographic and lesion characteristics on AAT performance*

Age was observed to have negative correlations for the average AAT performance and for all subscales (all $p < .01$) except the token test ($p = .06$). Sex was observed to have an influence solely on the subscale of auditory language comprehension with lower scores in males; $t(57) = 2.2$; $p = .03$. Higher WHO grade was significantly related to reduced AAT performance on the average AAT measure, as well as on the individual subscales (all $F > 3.2$, all $ps < .05$). Post-Hoc tests confirmed differences in the comparisons between WHO grade IV and grades III and IV vs II on all AAT subtests (all $ps < .03$) with grade WHO grade IV patients being more impaired. In light of these results (Table 2), WHO classification and patient age were added as covariates in VLSM analyses of all subscales. WHO grading was defined as a binary covariate (WHO grade IV vs WHO grade III and II), according to results of the post-hoc comparisons between gradings. Sex was added as a further covariate for the auditory language comprehension exclusively. Due to an error in data recording for one patient, only AAT scores for composite Language Comprehension were given in that specific patient but results for specific written and auditory language comprehension were missing. This patient was hence excluded from AAT subscales (written and auditory) analysis.

3.3. VLSM

VLSM analysis indicated significant contribution of a posterior perisylvian cluster (cluster extent with corrected $p < .05 = 48.528$ cm^3), covering both WM and GM, to AAT performance averaged across subtests (Fig. 4). When considering individual AAT subtests, a substantial overlap between significant clusters for analysis of the token test, picture naming and language comprehension results could be observed in left posterior perisylvian clusters, whereas

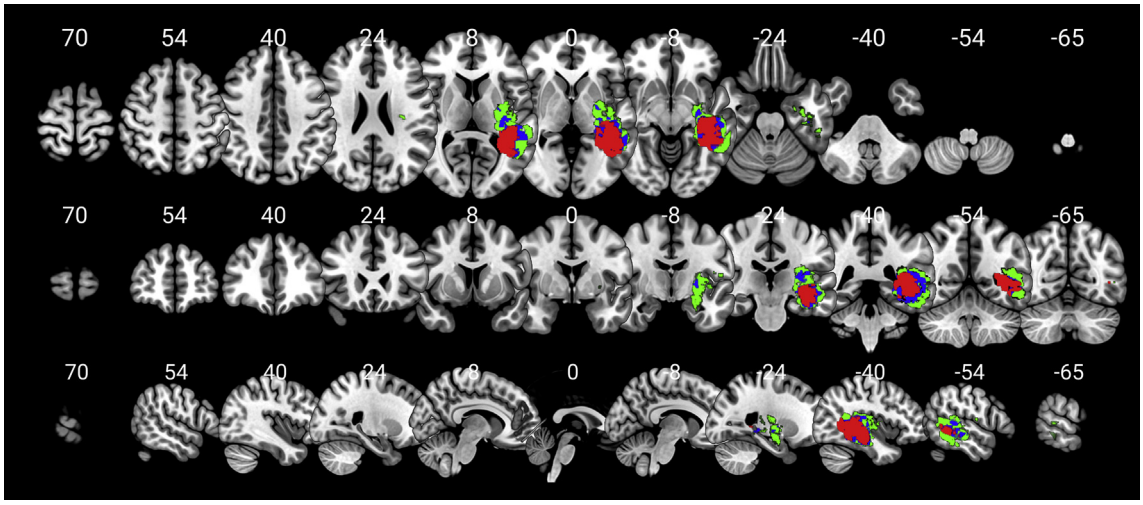

Fig. 4 – a. VLSM Voxel-wise correlates of AAT average t-scores with voxel-wise $p < .05$ (green), $p < .005$ (blue) and $p < .001$ (red) thresholds and a cluster-wise FWE-corrected $p < .05$ (cf. Fig. 4b for AAT subtests). The numbers above the slices indicate their axial slice positions in MNI space. b. VLSM Voxel-wise correlates of AAT subtests t-scores with voxel-wise $p < .05$ (green), $p < .005$ (blue) and $p < .001$ (red) thresholds and a cluster-wise FWE-corrected $p < .05$ (cf. Fig. 4b for AAT subtests). The numbers above the slices indicate their axial slice positions in MNI space.

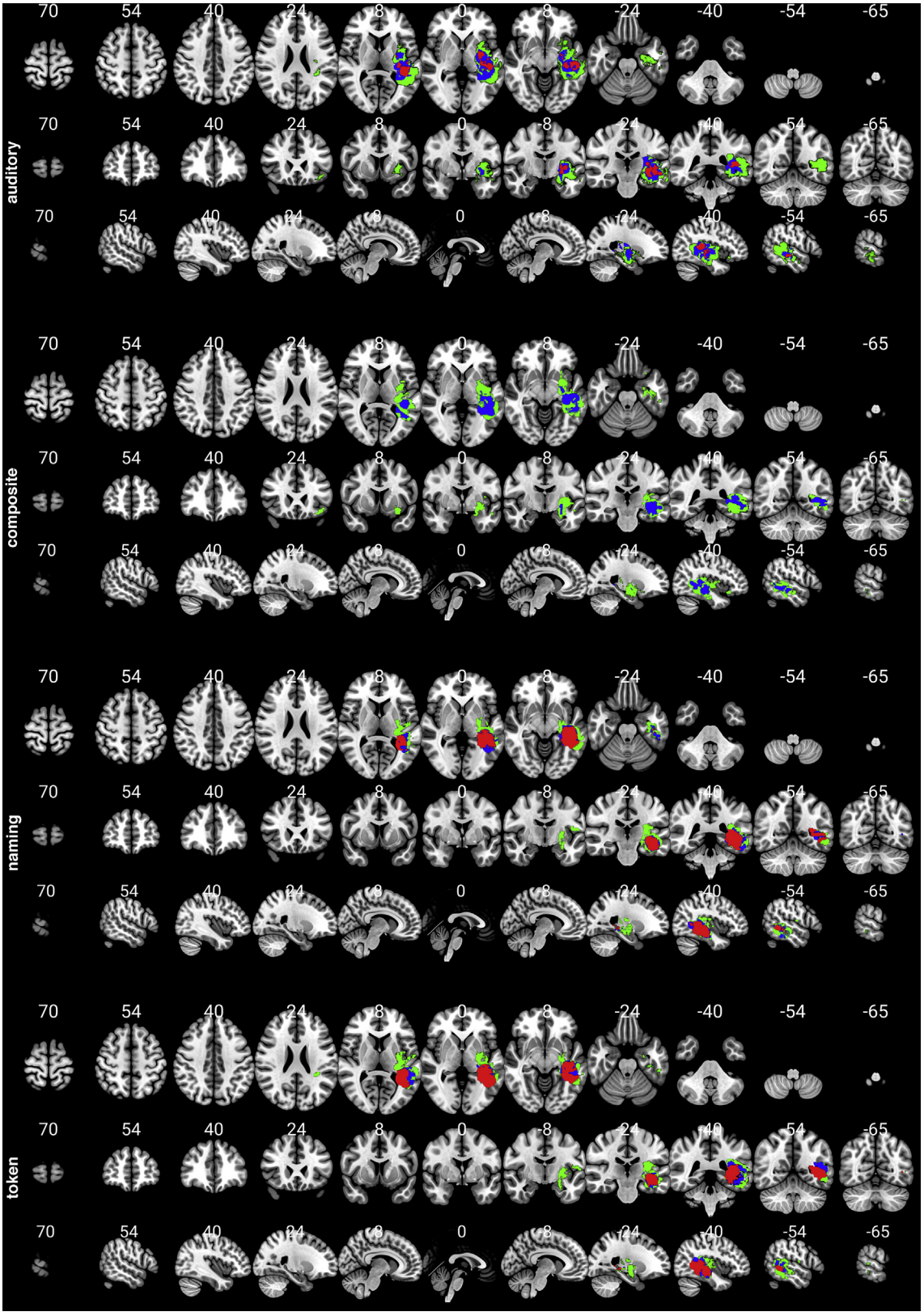

Fig. 4 – continued

Table 2 – Influence of sociodemographic and lesion characteristics on AAT results.

AAT scores	Age (Pearson r)	WHO Grade (ANOVA)	Sex (t-test)
Token test	-.24, $p = .059$	$F(2,57) = 1.91$, $p = .158$	$t(58) = .24$, $p = .81$
Verbal repetition	-.37, $p = .003$	$F(2,57) = 1.66$, $p = .2$	$t(58) = 1.16$, $p = .248$
Naming	-.39, $p = .002$	$F(2,57) = 1.9$, $p = .15$	$t(58) = 1.08$, $p = .286$
Language comprehension (composite)	-.45, $p < .001$	$F(2,57) = 4.09$, $p = .022$	$t(58) = 1.95$, $p = .056$
Language comprehension (auditory)	-.45, $p < .001$	$F(2,56) = 3.47$, $p = .037$	$t(57) = 2.2$, $p = .032$
Language comprehension (reading)	-.33, $p = .009$	$F(2,56) = 2.94$, $p = .061$	$t(57) = 1.72$, $p = .091$
Average across subscales	-.45, $p < .001$	$F(2,57) = 3.23$, $p = .047$	$t(58) = 1.41$, $p = .162$

Table 3a – Overlap volumes and ratios between each fiber bundle of IIT atlas and VLSM results.

	volFB (mm^3)	Average across subscales		Token test		Language comprehension (auditory)		Language comprehension (composite)		Naming	
		volOFB (mm^3)	CR (%)	volOFB (mm^3)	CR (%)	volOFB (mm^3)	CR (%)	volOFB (mm^3)	CR (%)	volOFB (mm^3)	CR (%)
AC	24,567	2336	15.0	2051	13.2	2523	16.2	2329	14.9	2468	15.8
AF	54,795	6545	19.3	6377	18.8	5627	16.6	5155	15.2	5347	15.8
AST	56,558	72	.2	40	.1	126	.3	39	.1	14	.0
CCMid	185,056	292	.2	414	.3	475	.4	135	.1	218	.2
CC_FMa	79,813	572	1.1	651	1.2	620	1.2	547	1.0	572	1.1
CC	442,246	14,850	5.2	14,695	5.1	15,950	5.5	13,025	4.5	13,232	4.6
CST	61,850	2185	4.9	2073	4.7	2809	6.3	1060	2.4	1767	4.0
FPT	82,140	1061	1.9	795	1.4	1447	2.6	330	.6	744	1.4
IFOF	15,383	3426	29.5	3293	28.4	3583	30.9	3631	31.3	3431	29.6
ILF	58,002	12,029	35.2	11,493	33.6	12,546	36.7	11,436	33.5	11,426	33.5
ML	38,686	184	1.1	144	.8	384	2.2	196	1.1	168	1.0
MdLF	37,411	9414	36.4	9479	36.6	10,247	39.6	7908	30.6	7911	30.6
OPT	42,272	3875	12.1	3909	12.2	4514	14.1	2720	8.5	3464	10.8
OR	35,089	8231	37.4	7850	35.6	8729	39.6	8033	36.5	8176	37.1
PPT	65,297	2720	5.8	2687	5.8	3421	7.3	1530	3.3	2292	4.9
SCP	82,910	657	1.8	618	1.7	834	2.3	498	1.4	626	1.7
SLF	79,260	1619	3.4	1445	3.1	1633	3.5	564	1.2	685	1.5
STT	53,789	377	1.6	301	1.3	643	2.7	369	1.6	377	1.6
UF	16,762	1144	13.4	980	11.5	2012	23.6	1439	16.9	1315	15.4
VOF	31,883	3022	18.2	3018	18.2	1809	10.9	2736	16.5	2981	17.9

volFB: Volume of fiber bundle; volOFB: Volume of overlap between fiber bundle and VLSM result; CR: Coverage ratio: VolOFB/volFB. AC: Anterior commissure; AF: Arcuate fasciculus; AST: Frontal aslant tract; CCMid: Middle of corpus callosum; CC_FMa: Forceps major; CC: Corpus callosum; CST: Left corticospinal tract; FPT: Frontopontine tract; IFOF: Inferior frontooccipital fasciculus; ILF: Inferior longitudinal fasciculus; ML: Medial lemniscus; MdLF: Middle longitudinal fasciculus; OPT: Occipitopontine tract; OR: Optic radiation; PPT: Parietopontine tract; SCP: Superior cerebellar peduncle; SLF: Superior longitudinal fasciculus; STT: Spinothalamic tract; UF: Uncinate fasciculus; VOF: Vertical occipital fasciculus.

analysis of the subtest for verbal repetition did not yield significant clusters after FWE-correction.

3.4. *White and grey matter involvement*

Especially optic radiation (OR, 37.4%), middle longitudinal fasciculus (MdLF, 36.4%), inferior longitudinal fasciculus (IFL, 35.2%), inferior fronto-occipital (IFOF, 29.5%) and arcuate fascicles (AF, 19.3%) derived from the WM and GM atlases (cf. 2.7) show high percentages of volumes of tract involvements in the VLSM on AAT results averaged across subscales. These findings show a major involvement (see red area in Fig. 4) of white matter underlying the middle and posterior parts of the temporal cortex, extending from Heschl's gyrus ($y = -20$) in posterior direction up to the visual word form area ($y = -55$), thus covering main sites relevant for language processing (Table 3a, Table 4 and Fig. 4).

In addition to above mentioned large portions of VLSM clusters of WM structures, our results delineate that multiple left cortical and subcortical GM areas are involved. Especially Heschl's gyrus (HESCHLL, 63.8%), also known as transverse temporal gyri, Hippocampus (HIPPOL, 38.5%), middle temporal gyrus (T2L, 34.4%), putamen (PUTL, 23.9%) and AAL3 derived Rolandic operculum [ORL, 20.2% (partially covering BA's 4, 6, 13, 22, 40, 41, 42, 43, 44)] demonstrate high percentages of intersections with the VLSM clusters for the analysis of average AAT t-scores, cf. Table 3b, Table 4 and Fig. 4. These involved cortical und subcortical GM areas may indicate that posterior perisylvian GM are central for language functions in tumor patients. Such a functional contribution of GM could be complementary to the above stated WM function, or the two could each be the single decisive factor. Post-hoc comparisons using a two-sample *t*-test with Bonferroni-Holm correction indicated that the mean scores of AAT t-scores between

Table 3b – Overlap volumes and ratios between each cortical area of AAL3 atlas and VLSM results.

	volCA (mm^3)	Average across subscales		Token test		Language comprehension (auditory)		Language comprehension (composite)		Naming	
		volOCA (mm^3)	CR (%)	volOCA (mm^3)	CR (%)	volOCA (mm^3)	CR (%)	volOCA (mm^3)	CR (%)	volOFB (mm^3)	CR (%)
F3O_2L	5261	0	0	0	0	135	2.6	118	2.2	0	0
ORL	6866	1388	20.2	1379	20.1	1834	26.7	349	5.1	1045	15.2
OFCPOSTL	4301	0	0	0	0	282	6.6	416	9.7	0	0
INL	13,657	2255	16.5	1641	12	5553	40.7	2608	19.1	936	6.9
HIPPOL	7165	2757	38.5	2176	30.4	4064	56.7	2428	33.9	2845	39.7
PARA_HIPPOL	6786	417	6.1	532	7.8	572	8.4	390	5.7	661	9.7
AMYGDL	1713	175	10.2	96	5.6	456	26.6	480	28.0	20	1.2
FUSIL	16,725	549	3.3	520	3.1	882	5.3	687	4.1	788	4.7
PUTL	6831	1635	23.9	1174	17.2	2887	42.3	1879	27.5	871	12.8
PALLL	1885	228	12.1	247	13.1	316	16.8	238	12.6	153	8.1
HESCHLL	1621	1034	63.8	978	60.3	1177	72.6	678	41.8	722	44.5
T1L	13,730	2657	19.4	2621	19.1	5151	37.5	1818	13.2	1290	9.4
T2L	32,143	8227	25.6	7073	22.0	9302	28.9	6091	18.9	5692	17.7
T3L	22,390	2638	11.8	2540	11.3	1154	5.2	1807	8.1	3386	15.1

volCA: Volume of cortical area; volOCA: Volume of overlap between cortical area and VLSM results; CR: Coverage ratio: volOCA/volCA. F3O_2L: Inferior frontal gyrus, orbital part; OFCPOSTL: Left posterior orbital gyrus; ORL: Left rolandic operculum; INL: Left insular; HIPPOL: Left hippocampus; PARA_HIPPOL: Left parahippocampal gyrus; AMYGDL: Amygdala; FUSIL: Left fusiform gyrus; PUTL: Left putamen; PALLL: Left Pallidum; HESCHLL: Left heschl's gyrus; T1L: Left superior temporal gyrus; T2L: Left middle temporal gyrus; T3L: Left inferior temporal gyrus.

lesioned and non-lesioned groups were significantly different in various GM areas (left inferior temporal gyrus, hippocampus and fusiform gyrus) and WM tracts (arcuate fascicle, forceps major, middle longitudinal fasciculus, optic radiation, parietopontine tract and superior cerebellar peduncle; see Table 4, Fig. 5 for details).

4. Discussion

Our VLSM analysis indicated a significant contribution of the posterior perisylvian network, in particular posterior temporal loci and in the related WM, to AAT performance averaged across subtests and covering both, GM and WM areas. We observed a substantial overlap between significant clusters for analysis of individual AAT subscales probing language comprehension, object naming and the token test. The WM-clusters are consistent with the overall importance of the long-range fiber bundles (including e.g., AF and IFOF) connecting the anterior and posterior parts of the perisylvian areas relevant for language function, along with that of posterior-temporal perisylvian GM (see Figs. 4 and 5). These pathways and areas are part of the macro-anatomical substrate of the language network (Friederici, 2011; Pulvermuller, 2013; Sarubbo et al., 2020; Schomers, Garagnani, & Pulvermuller, 2017).

The current VLSM findings show tumor induced lesions in left posterior perisylvian WM and GM clusters to be related to significant language impairments, as determined by the AAT. These findings correspond to results from earlier VLSM analyses of stroke patients. For example, in chronic post-stroke aphasia patients, analyses of language comprehension (Baldo & Dronkers, 2007; Bates et al., 2003; Bonilha et al., 2017) and picture naming performance (Baldo, Arevalo, Patterson, & Dronkers, 2013) revealed significant contributions of medial temporal areas in the left hemisphere. From an anatomical point of view, this region includes an intersection of terminations of dorsal and ventral pathways, such as the AF, ILF or IFOF, pointing out to adjacency and overlaps of both, streamlines from tractograms and cortical endings of these fiber bundles (Sarubbo et al., 2020). Likewise, VLSM on AAT language comprehension scores and object naming performance in acute stroke (Henseler, Regenbrecht, & Obrig, 2014) highlighted significant contributions of left middle temporal gyrus, but also of the left inferior frontal gyrus. The latter was only marginally reflected in the current GM findings by the involvement of the Rolandic operculum.

Nevertheless, our VLSM results do not suggest a role of BA44-45 (Broca's area) in AAT performance apart from auditory language comprehension (cf. Table 5). The absence of prominent inferior frontal GM is complementary to earlier studies in stroke patients (Bates et al., 2003) and direct electrical stimulation (DES) findings (Sarubbo et al., 2020; Tate, Herbet, Moritz-Gasser, Tate, & Duffau, 2014). The absence of inferior frontal GM clusters in the VLSM results is in line with previous observations on the absence of long lasting aphasia after resection of Broca's area (BA 44 and 45) (Duffau, 2018). A potential explanation for this observation may be seen in neuroplasticity processes, compensating for effects of brain tumor or specifically glioma related lesions on language performance, as it has been reported earlier (Amoruso et al., 2021; Piai et al., 2020; Yuan et al., 2020).

For stroke patients, it was recently shown that specifically lesions in left frontal areas led to lesion-homologous cortex involvement of the right hemisphere during language recovery throughout the acute, subacute and chronic stages (Stockert et al., 2020). This could possibly be interpreted as frontal areas, such as BA44-45, benefiting from contralateral plasticity to a larger degree than temporal areas, which in turn could be manifested in the dominance of the posterior perisylvian network with respect to the current VLSM results and language function. In strokes, the lesion occurs in minutes or

Table 4 – Comparisons of AAT t-scores between patients with and without a lesion in AAL ROIs and ITT tracts.

	Average across subscales			Token test			Verbal repetition			Naming			Language comprehension (composite)			Language comprehension (auditory)			Language comprehension (reading)		
	Mean T-score		p	Mean T-score		p	Mean T-score		p	Mean T-score		p	Mean T-score		p	Mean T-score		p	Mean T-score		p
	affected	Non-affected		affected	Non-affected		affected	Non-affected		affected	Non-affected		affected	Non-affected		affected	Non-affected		affected	Non-affected	
ORL	67.87	66.45	.502	69.75	67.22	.178	66.77	65.81	.630	66.96	67.92	.761	68.00	64.86	.313	67.25	61.71	.067	65.46	63.74	.559
INL	70.45	65.66	.034	69.82	67.60	.289	68.79	65.16	.017	71.59	65.93	.089	71.59	63.95	.020	72.06	60.69	.000	68.18	62.93	.103
HIPPOL	70.04	61.40	**.000***	70.46	64.10	.008	67.37	64.00	.086	72.67	58.00	**.000***	69.67	59.52	.002	67.29	57.95	.004	67.45	59.00	.005
PARA_HIPPOL	69.25	62.55	.006	69.65	65.40	.085	67.06	64.45	.184	71.18	60.25	.003	69.13	60.10	.010	67.13	57.80	.005	67.10	59.25	.013
AMYGDL	67.76	64.97	.245	68.80	66.69	.395	66.19	66.19	.997	68.77	64.13	.199	67.30	62.88	.225	65.35	60.25	.176	65.28	62.19	.333
LINGL	68.37	56.77	.010	69.11	61.57	.129	66.94	60.50	.102	69.81	50.29	.003	67.62	54.71	.037	65.38	53.43	.030	66.00	52.86	.019
O2L	67.83	61.72	.166	68.69	65.25	.415	67.11	60.25	.097	68.35	62.25	.368	67.19	59.13	.125	64.63	59.75	.286	65.55	57.38	.135
FUSIL	69.57	61.51	.001	69.95	64.53	.033	66.90	64.66	.264	72.00	57.89	**.000***	69.44	58.95	.003	67.48	56.58	.001	67.30	58.42	.004
PUTL	68.68	65.24	.094	69.03	67.38	.397	66.98	65.34	.382	69.26	65.69	.234	69.45	62.55	.019	68.03	59.46	.003	67.23	61.36	.029
PALLL	68.47	62.67	.035	69.00	65.93	.246	67.08	63.53	.153	68.96	63.27	.140	68.84	57.93	.004	67.00	55.07	.001	66.61	58.07	.009
HESCHLL	68.63	65.30	.106	70.35	65.97	.023	66.98	65.34	.379	68.61	66.38	.459	68.55	63.52	.090	67.06	60.54	.030	66.48	62.18	.111
T1L	69.18	66.30	.200	71.00	67.31	.038	66.50	66.09	.870	70.87	66.42	.114	68.33	65.38	.357	66.87	62.98	.232	66.60	63.70	.354
T2L	69.75	65.20	.018	71.58	66.00	.001	67.42	65.38	.292	71.33	65.00	.019	68.67	64.42	.138	66.88	61.97	.093	67.38	62.43	.066
T3L	69.79	62.56	.001	70.22	65.04	.019	67.14	64.67	.213	72.51	59.52	**.000***	69.30	61.00	.010	67.43	58.14	.004	67.11	59.95	.015
AC	70.16	65.07	.007	70.65	66.73	.027	67.50	65.38	.226	72.39	64.51	.003	70.09	63.65	.024	69.65	60.33	.002	67.43	62.53	.062
AF	71.50	66.78	.224	69.67	68.16	.737	71.00	65.94	**.000***	67.33	67.54	.980	78.00	65.49	**.000***	78.00	63.21	.002	74.33	63.91	.089
AST	65.74	67.66	.413	66.75	68.98	.302	65.48	66.55	.609	64.75	68.93	.239	66.00	66.18	.959	64.25	63.82	.895	63.90	64.72	.791
CCMid	NA	67.02	NA	NA	68.23	NA	NA	66.19	NA	NA	67.53	NA	NA	66.12	NA	NA	63.97	NA	NA	64.44	NA
CC_FMA	71.86	65.93	.002	71.36	67.53	.018	70.18	65.30	**.000***	72.27	66.47	.101	73.64	64.43	.008	71.55	62.23	.008	70.36	63.08	.023
CC	67.08	66.88	.930	67.79	69.28	.492	65.96	66.72	.728	67.05	68.67	.600	67.52	62.83	.163	65.44	60.61	.129	65.56	61.89	.241
CST	70.79	65.53	.010	71.06	67.12	.011	68.00	65.48	.241	73.29	65.26	.009	70.82	64.26	.042	68.38	62.33	.066	68.19	63.05	.085
FPT	68.06	66.50	.483	69.15	67.78	.484	66.85	65.86	.637	67.40	67.60	.955	68.85	64.75	.203	67.05	62.50	.161	65.95	63.73	.453
IFOF	71.08	65.14	.001	70.42	67.22	.064	68.47	65.13	.037	72.42	65.27	.009	73.00	62.93	.000	72.89	59.73	**.000***	69.84	61.88	.003
ILF	71.08	65.14	.005	70.42	67.22	.007	68.47	65.13	.318	72.42	65.27	.012	73.00	62.93	.007	72.89	59.73	.002	69.84	61.88	.008
ML	68.65	65.38	.110	68.77	67.70	.582	67.02	65.37	.377	69.43	65.63	.204	69.40	62.83	.025	67.90	60.17	.009	67.03	61.93	.060
MdLF	70.10	65.80	.030	72.18	66.67	**.000***	67.79	65.56	.303	71.88	65.81	.018	68.53	65.16	.283	66.71	62.86	.223	67.76	63.10	.131
OPT	71.35	64.13	**.000***	71.71	65.92	.001	68.96	64.35	.012	73.38	63.64	.000	71.38	62.61	.002	69.17	60.64	.003	68.61	61.78	.012
OR	70.20	65.30	.013	71.33	66.56	.004	67.14	65.68	.474	72.19	65.03	.007	70.14	63.95	.035	68.95	61.21	.011	68.43	62.24	.027
PPT	72.55	65.01	**.000***	71.44	67.07	.004	70.34	64.68	**.000***	74.50	65.00	.001	73.94	63.27	**.000***	71.33	61.45	.001	71.07	62.18	**.000***
SCP	73.04	65.96	**.000***	71.11	67.73	.060	70.28	65.47	**.000***	75.33	66.16	.015	75.44	64.47	.000	74.89	62.00	.000	71.78	63.12	.002
SLF	70.36	66.43	.050	70.67	67.80	.107	70.00	65.52	.000	68.11	67.43	.866	72.67	64.96	.048	70.56	62.78	.037	67.56	63.88	.253
STT	70.31	64.82	.003	69.71	67.25	.173	67.79	65.13	.133	72.13	64.47	.005	71.63	62.44	.001	70.25	59.66	.000	69.13	61.23	.002
UF	69.86	65.49	.020	69.48	67.56	.307	66.88	65.82	.545	72.24	65.00	.006	70.86	63.56	.009	69.76	60.76	.002	68.24	62.34	.025
VOF	70.32	63.49	.001	71.45	64.79	.001	67.74	64.53	.084	72.13	62.62	.001	69.97	62.00	.007	68.55	58.89	.001	67.84	60.68	.008

Cortical areas: ORL: Left rolandic operculum; INL: Left insular; HIPPOL: Left hippocampus; PARA_HIPPOL: Left parahippocampal gyrus; AMYGDL: Amygdala; LINGL: Left lingual gyrus; O2L: Left middle occipital gyrus; FUSIL: Left fusiform gyrus; PUTL: Left putamen; PALLL: Left Pallidum; HESCHLL: Left heschl's gyrus; T1L: Left superior temporal gyrus; T2L: Left middle temporal gyrus; T3L: Left inferior temporal gyrus.

Fiber bundles: AC: Anterior commissure; AF: Arcuate fasciculus; AST: Frontal aslant tract; CCMid: Middle of corpus callosum; CC_FMa: Forceps major; CC: Corpus callosum; CST: Left corticospinal tract; FPT: Frontopontine tract; IFOF: Inferior frontooccipital fasciculus; ILF: Inferior longitudinal fasciculus; ML: Medial lemniscus; MdLF: Middle longitudinal fasciculus; OPT: Occipitopontine tract; OR: Optic radiation; PPT: Parietopontine tract; SCP: Superior cerebellar peduncle; SLF: Superior longitudinal fasciculus; STT: Spinothalamic tract; UF: Uncinate fasciculus; VOF: Vertical occipital fasciculus.

The alpha level was changed to .000174 after Bonferroni-Holm correction and only p values < .000174 were determined as significant.

Boldface and asterisks represent significant differences.

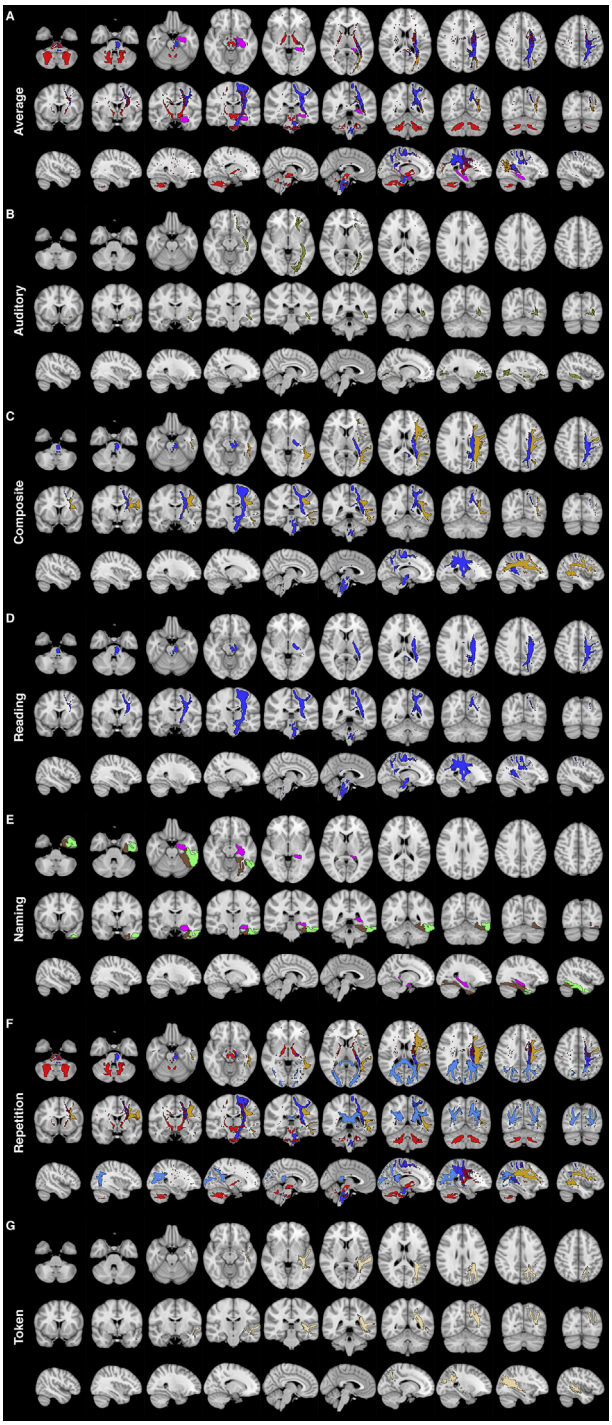

Fig. 5 – WM and GM areas that show significant differences of AAT t-scores with subscales (A–G) between lesioned and non-lesioned groups. The colors indicate the various IIT-derived fiber bundles and AAL3-based GM regions [AF: yellow (dark); CC_FMA: blue; FUSIL: dark brown; HIPPOL: pink; IFOF: dark green MdLF: yellow (light); OPT: orange; PPT: dark blue; SCP: red; T3L: green].

hours. By contrast, gliomas develop slower, with an estimated age of roughly a year, depending on the tumor volume at diagnosis and its genetic profile (Stensjoen, Berntsen, Jakola, & Solheim, 2018). The slower growth leaves more time for neural compensation mechanisms to take effect and thus may result in even stronger compensation of inferior frontal lesion as found in stroke patients. Likewise, the independence from vascular properties of gliomas and the resulting higher focality of these lesions may have left certain components of the language network intact when compared with strokes, potentially facilitating neuroplastic compensation for local processing deficits. Also consistent with our results, current language models suggest a strongly connected posterior perisylvian hub area of language function, which may be further reflected in our results by the strong WM relationships to the VLSM findings (see Fig. 4) (Ius, Angelini, Thiebaut de Schotten, Mandonnet, & Duffau, 2011; Tuncer et al., 2021). Therefore, the current findings seem consistent with a connectomal framework in which cerebral processing is not conceived as the sum of segregated subfunctions but results from network integration and potentiation of parallel subcircuits that have the potential for network-wide reorganization processes to compensate for focal lesions within the related network and indicates that subcortical plasticity may be rather low (Duffau, 2015; Ius et al., 2011).

In a similar vein the apparent key role of posterior perisylvian sites may not just depend on GM lesions, but on damage of the underlying WM connections as well (Duffau, 2018; Plaza, Gatignol, Leroy, & Duffau, 2009; Tate et al., 2014), which in turn could also impair the aforementioned network-wide compensation mechanisms processes.

Neuroplasticity compensating for effects of glioma lesions on language performance may also explain a further observation in the current results: The overall well-preserved language function throughout this cohort of glioma patients. According to the AAT results, only 11.7% of patients exhibited moderate and another 11.7% mild aphasia symptoms, which is less severe than typically observed for cohorts of stroke patients with similar lesion profiles (Bates et al., 2003; Henseler et al., 2014). The overview of voxel-wise average AAT t-scores for patients with a lesion in a given voxel indicates only very mild impairments across the cohort (see Fig. 4). This observation is of potential clinical relevance and provides evidence for the feasibility of pre-operative and intra-operative language mapping procedures even in patients with gliomas within areas related to language processing in general and picture naming in particular. However, attributing the difference solely to increased compensating neuroplasticity in glioma compared to stroke patients might be most convincing for low-grade gliomas, but not to the same degree for WHO grade IV glioblastomas, which constitute 53% of the patient sample. WHO grade IV glioblastomas are fast growing, aggressive and highly malignant tumor and thus leave less time for compensating neuroplasticity to take place. The pre-selection of patients in the present context of awake testing during neurosurgery constitutes a selection criterion that tends to favor patients without substantial cognitive deficits and, to a degree, still functional language. This indicates that our finding of a relatively low proportion of aphasics and complete absence of severe aphasics therefore requires confirmation by future work.

Our present results obtained in tumor patients with sometimes very small and focal lesions allow us to draw some

Table 5 – Affected Brodmann areas by VLSM results.

	Max t-scores of clusters (MNI coordinates)			Cluster volume (mm^3)	Affected Brodmann areas
	x	y	z		
Average across subscales	−42	−38	6	48,528	BA 13, BA19, BA 20, BA 21, BA 22, BA 36, BA 37, BA 41, BA 42, BA 43
Token test	−31	−38	6	44,096	BA 13, BA19, BA 20, BA 21, BA 22, BA 35, BA 36, BA 37, BA 39, BA 41, BA 42, BA 43
Naming	−41	−22	−13	40,110	BA 13, BA19, BA 20, BA 21, BA 22, BA 28, BA 35, BA 36, BA 37, BA 39, BA 41, BA 43
Language comprehension (composite)	−33	−24	−2	41,708	BA 13, BA19, BA 20, BA 21, BA 22, BA 35, BA 36, BA 37, BA 39, BA 41, BA 47
Language comprehension (auditory)	−43	−26	0	60,953	BA 13, BA 20, BA 21, BA 22, BA 28, BA 34, BA 35, BA 36, BA 37, BA 39, BA 40, BA 41, BA 42, BA 44, BA 47

tentative conclusions on the precise loci of lesions causing relevant linguistic deficits. The major lesion loci entailing severe reduction of AAT scores were seen in the posterior temporal subcortical area, encompassing also some overlaying GM in this location. The lesioned core area (see red area in Fig. 4) included the underlying WM of all three temporal gyri, approximately between the y coordinate of Heschl's gyrus and that of the so-called visual word form area (i.e., from y = −20 to −55). This area is seen as important for language not only because it channels visual and auditory information relevant for linguistic perception, but also because it houses most of the WM tracts interlinking areas of the language network of the left-perisylvian cortex. Not only the AF, but also the extreme capsule and its related fiber bundles encompass this area, and the lesion of these fiber tracts provides an obvious candidate explanation for its relevance. It could also be that lesioned GM made a significant contribution to the lesion profile and causation of aphasia syndromes, as posterior STG and MTG along with the visual word form area in posterior inferior temporal gyrus are well known sites important for different aspects of language processing. However, our results are also consistent with a role of the so-called *semantic hub* in the anterior temporal cortex. In the context of research on semantic dementia, which includes severe deficits in naming and conceptual processing, it has been argued that an anterior temporal fusiform center is crucial for processing of meaning, and that this area is consequently critically involved in language understanding and naming (Patterson, Nestor, & Rogers, 2007; Ralph, Jefferies, Patterson, & Rogers, 2017). Language comprehension and naming were targets of most of the tests applied in this study, and, in the left hemisphere, the anterior temporal semantic hub is currently estimated to center around y coordinate −25 (Mion et al., 2010), thus lying close to the anterior end of the most severely affected area in the present cohort.

The underlying WM revealed to be related to language comprehension and picture naming in the current analysis also shows correspondence to results on the neural bases of semantic processing from combined fMRI and diffusion weighted imaging analyses in healthy participants (Saur et al., 2008, 2010).

Our study did not provide strong support for effects on language exerted by tumors affecting the frontal or parietal cortex or their related subcortical structures. As already mentioned, this may be due in part to the relative sparseness of such lesions in our sample (Fig. 1) and to the fact that many frontal lesions were rather large (Fig. 2). However, the power map (Fig. 3) indicates sufficient voxel-wise statistical power for VLSM analysis at least in temporal cortices, the insula and inferior frontal areas. The observed rareness of frontal impact on language (comprehension) contrasts with previous evidence for a functional role of these areas in semantic processing, as found in stroke (Arevalo, Baldo, & Dronkers, 2012; Neininger & Pulvermuller, 2003) and brain tumor patients (Dreyer et al., 2015; Dreyer, Picht, Frey, Vajkoczy, & Pulvermuller, 2020).

The predominant role of temporal areas emerging from this work may also be due, in part, to the test's predominant use of language that closely relates to objects and visual perceptions. Not only the Token Test probes knowledge about correspondence between colors and shapes and the related symbols, also the naming and comprehension tests applied target the relationship between (pictures of) objects and words or phrases. It may be that a broader coverage of semantics, including e.g., foci on language about spatial relationship, action and social interaction, could help reveal a contribution of other areas too.

The large amount of involved WM, indicating a broadly affected network, is in line with current language network models (Friederici & Gierhan, 2013) and may even point to a causal and functional involvement of further cerebral structures into language processing, responsible for a wide range of processes such as cognitive functions (Pulvermuller, 2018). In particular, VLSM results in the AF and IFOF resonate with earlier findings on their relevance for language functions from intraoperative electrical stimulation approaches in glioma patients (Duffau et al., 2002, 2005). In addition, the existence of multiple fiber populations per voxel led to a strong

involvement of the OR which passes through the identified voxels as revealed by VLSM in the present study. However, a functional involvement was not confirmed by impairments of the patients' visual capability and this finding is highly likely related to the relatively low resolution in relation to WM microarchitecture.

Similar to the involvement of the OR, the MdLF might not be a primary connection for language processing, it is rather suspected that the MdLF is involved in a parallel transmodal neurocognitive network (De Witt Hamer, Moritz-Gasser, Gatignol, & Duffau, 2011; Menjot de Champfleur et al., 2013). Thus, the reported high percentages of OR and MdLF involvement in significant VLSM clusters may be a by-product of their anatomical proximity to the perisylvian language network.

Likewise, earlier intraoperative DES investigations on glioma patients did also not indicate that the ILF is indispensable for language (Mandonnet, Nouet, Gatignol, Capelle, & Duffau, 2007), thus leaving the possibility of VLSM findings in this tract may also not be causal for language deficits in the present cohort. However, a recent study highlights subcortical DES with a high frequency of subcortical anomia at the junction below the posterior temporal cortices (STG and MTG) and the inferior parietal lobule, as well as cortical and subcortical distributions of semantic paraphasias (Sarubbo et al., 2020). In fact, due to overlaps of multiple fiber bundles per voxel, the individual contribution of a specific tract cannot be disentangled.

Moreover, as can be seen descriptively from the comparison between the average size of the lesions and the VLSM results, the location of the lesion rather than the lesion volume in relation to the network seems to be responsible for the effects as lesions in the frontal lobe were larger but were not associated with more pronounced deficits.

The current VLSM study partly confirms findings of an earlier VLSM analysis on language performance in glioma patients (Banerjee et al., 2015). In their study, Banerjee et al. reported language comprehension performance to be significantly impaired in patients with gliomas in temporal and subcortical regions. Interestingly, their findings also did not demonstrate a consistent involvement of inferior-frontal or Broca's area in relation to expressive language functions. In contrast to the current approach, the patient sample of Banerjee et al. included patients following resection and radio- and/or chemotherapy. Although these patient characteristics were added as covariates in the analysis, their VLSM approach still treated resections in a given voxel like a voxel containing tumorous tissue or edema in another patient. This procedure appears to be problematic regarding the inferences that may be drawn from such an analysis, as tumor or edema in a voxel may allow for residual neuronal functionality whereas actual resection does not. We therefore believe that our alternative results derived from a retrospective cohort, along with the partially different results presented here, require further investigation and possible confirmation.

5. Limitations

Patients investigated in the current retrospective analysis received AAT testing in the context of preoperative TMS language mappings, based on an object naming task. In case a patient was not considered for TMS language mappings (e.g., because of language impairments being too severe to perform a naming task) also the AAT was unfortunately not performed. This may have led to an implicit bias in sampling for patients with better general language performance or better language production capabilities (thus possibly limiting the ecological validity of our findings). In agreement with this, our study did not include any patients with severe aphasia, although a significant proportion of left-hemisphere lesioned patients normally fall in this category. A further bias may have led to favoring of patients with temporal lesions. Although language deficits are common in patients with frontal and temporal lesions, the additional occurrence of motor deficits may have led to an exclusion of more patients with frontoparietal tumors, thus possibly accounting, in part, for the great overlap of temporal lobe lesioned tissue (Fig. 1). This consideration could also explain that our VLSM analysis of the verbal repetition subtest did not reveal any significant clusters, as patients with deficits in this domain might not have been included in the database. Since patients excluded prior to pre-operative language examination were also absent from the database this study is based on, we can only speculate on the influence such a selection bias may have had on our findings, but have no means to test this directly. This would require a subsequent prospective study collecting AAT measures in glioma patients independent of their language capabilities. However, this is beyond the scope of this retrospective analysis. Moreover, the AAT could have underestimated language deficits in low grade gliomas, as it has originally been designed and validated for language assessment in stroke patients.

Furthermore, our results regarding GM and WM involvements are atlas dependent since other atlas choices would result in different parcellations. In addition, the exact tumor infiltration may not be differentiated, especially in low grade gliomas and thus could pose a limitation of the spatial resolution of lesion masking.

Credits

Lucius Samo Fekonja: Conceptualization, Methodology, Software, Visualization, Investigation, Writing - Original Draft, Writing - Review & Editing. **Ziqian Wang:** Methodology, Software, Investigation, Writing - Original Draft. **Lea Doppelbauer:** Methodology, Software, Investigation. **Peter Vajkoczy:** Resources, Supervision, Writing - Original Draft, Writing - Review & Editing. **Thomas Picht:** Conceptualization, Resources, Supervision, Writing - Original Draft, Writing - Review & Editing. **Friedemann Pulvermüller:** Supervision, Writing - Original Draft, Writing - Review & Editing. **Felix R. Dreyer:** Conceptualization, Methodology, Software, Supervision, Investigation, Writing - Original Draft, Writing - Review & Editing.

Pre-registration information

No part of the study procedures was pre-registered prior to the research being conducted. No part of the study analyses was pre-registered prior to the research being conducted.

Funding

LF, TP, FP acknowledge the support of the Cluster of Excellence *Matters of Activity. Image Space Material* funded by the Deutsche Forschungsgemeinschaft (DFG, German Research Foundation) under Germany's Excellence Strategy – EXC 2025–390648296.

Declaration of competing interest

The authors report no competing interests.

REFERENCES

Amoruso, L., Geng, S., Molinaro, N., Timofeeva, P., Gisbert-Munoz, S., Gil-Robles, S., … Carreiras, M. (2021). Oscillatory and structural signatures of language plasticity in brain tumor patients: A longitudinal study. *Human Brain Mapping, 42*(6), 1777–1793. https://doi.org/10.1002/hbm.25328

Arevalo, A. L., Baldo, J. V., & Dronkers, N. F. (2012). What do brain lesions tell us about theories of embodied semantics and the human mirror neuron system? *Cortex, 48*(2), 242–254. https://doi.org/10.1016/j.cortex.2010.06.001

Avants, B. B., Tustison, N. J., Song, G., Cook, P. A., Klein, A., & Gee, J. C. (2011). A reproducible evaluation of ANTs similarity metric performance in brain image registration. *Neuroimage, 54*(3), 2033–2044. https://doi.org/10.1016/j.neuroimage.2010.09.025

Baldo, J. V., Arevalo, A., Patterson, J. P., & Dronkers, N. F. (2013). Grey and white matter correlates of picture naming: Evidence from a voxel-based lesion analysis of the boston naming test. *Cortex, 49*(3), 658–667. https://doi.org/10.1016/j.cortex.2012.03.001

Baldo, J. V., & Dronkers, N. F. (2007). Neural correlates of arithmetic and Language comprehension: A common substrate? *Neuropsychologia, 45*(2), 229–235. https://doi.org/10.1016/j.neuropsychologia.2006.07.014

Banerjee, P., Leu, K., Harris, R. J., Cloughesy, T. F., Lai, A., Nghiemphu, P. L., … Ellingson, B. M. (2015). Association between lesion location and language function in adult glioma using voxel-based lesion-symptom mapping. *Neuroimage Clinical, 9*, 617–624. https://doi.org/10.1016/j.nicl.2015.10.010

Bates, E., Wilson, S. M., Saygin, A. P., Dick, F., Sereno, M. I., Knight, R. T., et al. (2003). Voxel-based lesion-symptom mapping. *Nature Neuroscience, 6*(5), 448–450. https://doi.org/10.1038/nn1050

Bonilha, L., Hillis, A. E., Hickok, G., den Ouden, D. B., Rorden, C., & Fridriksson, J. (2017). Temporal lobe networks supporting the comprehension of spoken words. *Brain: a Journal of Neurology, 140*(9), 2370–2380. https://doi.org/10.1093/brain/awx169

De Witt Hamer, P. C., Moritz-Gasser, S., Gatignol, P., & Duffau, H. (2011). Is the human left middle longitudinal fascicle essential for language? A brain electrostimulation study. *Human Brain Mapping, 32*(6), 962–973. https://doi.org/10.1002/hbm.21082

Dreyer, F. R., Frey, D., Arana, S., von Saldern, S., Picht, T., Vajkoczy, P., et al. (2015). Is the motor system necessary for processing action and abstract emotion words? Evidence from focal brain lesions. *Frontiers in Psychology, 6*, 1661. https://doi.org/10.3389/fpsyg.2015.01661

Dreyer, F. R., Picht, T., Frey, D., Vajkoczy, P., & Pulvermuller, F. (2020). The functional relevance of dorsal motor systems for processing tool nouns- evidence from patients with focal lesions. *Neuropsychologia, 141*, 107384. https://doi.org/10.1016/j.neuropsychologia.2020.107384

Duffau, H. (2015). Stimulation mapping of white matter tracts to study brain functional connectivity. *Nature Reviews. Neurology, 11*(5), 255–265. https://doi.org/10.1038/nrneurol.2015.51

Duffau, H. (2018). The error of Broca: From the traditional localizationist concept to a connectomal anatomy of human brain. *Journal of Chemical Neuroanatomy, 89*, 73–81. https://doi.org/10.1016/j.jchemneu.2017.04.003

Duffau, H., Capelle, L., Sichez, N., Denvil, D., Lopes, M., Sichez, J. P., … Fohanno, D. (2002). Intraoperative mapping of the subcortical language pathways using direct stimulations. An anatomo-functional study. *Brain: a Journal of Neurology, 125*(Pt 1), 199–214. Retrieved from https://www.ncbi.nlm.nih.gov/pubmed/11834604.

Duffau, H., Gatignol, P., Mandonnet, E., Peruzzi, P., Tzourio-Mazoyer, N., & Capelle, L. (2005). New insights into the anatomo-functional connectivity of the semantic system: A study using cortico-subcortical electrostimulations. *Brain: a Journal of Neurology, 128*(Pt 4), 797–810. https://doi.org/10.1093/brain/awh423

Friederici, A. D. (2011). The brain basis of language processing: From structure to function. *Physiological Reviews, 91*(4), 1357–1392. https://doi.org/10.1152/physrev.00006.2011

Friederici, A. D., & Gierhan, S. M. (2013). The language network. *Current Opinion in Neurobiology, 23*(2), 250–254. https://doi.org/10.1016/j.conb.2012.10.002

Garyfallidis, E., Cote, M. A., Rheault, F., Sidhu, J., Hau, J., Petit, L., … Descoteaux, M. (2018). Recognition of white matter bundles using local and global streamline-based registration and clustering. *Neuroimage, 170*, 283–295. https://doi.org/10.1016/j.neuroimage.2017.07.015

Grabner, G., Janke, A. L., Budge, M. M., Smith, D., Pruessner, J., & Collins, D. L. (2006). Symmetric atlasing and model based segmentation: An application to the hippocampus in older adults. *Medical Image Computing and Computer-assisted Intervention: MICCAI ., 9*(Pt 2), 58–66. Retrieved from https://www.ncbi.nlm.nih.gov/pubmed/17354756.

Henseler, I., Regenbrecht, F., & Obrig, H. (2014). Lesion correlates of patholinguistic profiles in chronic aphasia: Comparisons of syndrome-, modality- and symptom-level assessment. *Brain: a Journal of Neurology, 137*(Pt 3), 918–930. https://doi.org/10.1093/brain/awt374

Herbet, G., Lafargue, G., & Duffau, H. (2015). Rethinking voxel-wise lesion-deficit analysis: A new challenge for computational neuropsychology. *Cortex, 64*, 413–416. https://doi.org/10.1016/j.cortex.2014.10.021

Hilari, K., & Byng, S. (2009). Health-related quality of life in people with severe aphasia. *International Journal of Language & Communication Disorders, 44*(2), 193–205. https://doi.org/10.1080/13682820802008820

Huber, W., Poeck, K., & Willmes, K. (1984). The aachen aphasia test. *Advances in Neurology, 42*, 291–303. Retrieved from https://www.ncbi.nlm.nih.gov/pubmed/6209953.

Ius, T., Angelini, E., Thiebaut de Schotten, M., Mandonnet, E., & Duffau, H. (2011). Evidence for potentials and limitations of brain plasticity using an atlas of functional resectability of WHO grade II gliomas: Towards a "minimal common brain". *Neuroimage, 56*(3), 992–1000. https://doi.org/10.1016/j.neuroimage.2011.03.022

Jenkinson, M., Beckmann, C. F., Behrens, T. E., Woolrich, M. W., & Smith, S. M. (2012). *The Florida Nurse, 62*(2), 782–790. https://doi.org/10.1016/j.neuroimage.2011.09.015

Mandonnet, E., Nouet, A., Gatignol, P., Capelle, L., & Duffau, H. (2007). Does the left inferior longitudinal fasciculus play a role in language? A brain stimulation study. *Brain: a Journal of Neurology, 130*(Pt 3), 623–629. https://doi.org/10.1093/brain/awl361

Menjot de Champfleur, N., Lima Maldonado, I., Moritz-Gasser, S., Machi, P., Le Bars, E., Bonafe, A., et al. (2013). Middle

longitudinal fasciculus delineation within language pathways: A diffusion tensor imaging study in human. *European Journal of Radiology, 82*(1), 151–157. https://doi.org/10.1016/j.ejrad.2012.05.034

Mion, M., Patterson, K., Acosta-Cabronero, J., Pengas, G., Izquierdo-Garcia, D., Hong, Y. T., … Nestor, P. J. (2010). What the left and right anterior fusiform gyri tell us about semantic memory. *Brain: A Journal of Neurology, 133*(11), 3256–3268. https://doi.org/10.1093/brain/awq272

Neininger, B., & Pulvermuller, F. (2003). Word-category specific deficits after lesions in the right hemisphere. *Neuropsychologia, 41*(1), 53–70. https://doi.org/10.1016/s0028-3932(02)00126-4

Oldfield, R. C. (1971). The assessment and analysis of handedness: The Edinburgh inventory. *Neuropsychologia, 9*(1), 97–113. https://doi.org/10.1016/0028-3932(71)90067-4

Patterson, K., Nestor, P. J., & Rogers, T. T. (2007). Where do you know what you know? The representation of semantic knowledge in the human brain. *Nature Reviews. Neuroscience, 8*(12), 976–987. https://doi.org/10.1038/nrn2277

Piai, V., De Witte, E., Sierpowska, J., Zheng, X., Hinkley, L. B., Mizuiri, D., … Nagarajan, S. S. (2020). Language neuroplasticity in brain tumor patients revealed by magnetoencephalography. *Journal of Cognitive Neuroscience, 32*(8), 1497–1507. https://doi.org/10.1162/jocn_a_01561

Plaza, M., Gatignol, P., Leroy, M., & Duffau, H. (2009). Speaking without Broca's area after tumor resection. *Neurocase, 15*(4), 294–310. https://doi.org/10.1080/13554790902729473

Pulvermuller, F. (2013). How neurons make meaning: Brain mechanisms for embodied and abstract-symbolic semantics. *Trends in Cognitive Sciences, 17*(9), 458–470. https://doi.org/10.1016/j.tics.2013.06.004

Pulvermuller, F. (2018). Neural reuse of action perception circuits for language, concepts and communication. *Progress in Neurobiology, 160*, 1–44. https://doi.org/10.1016/j.pneurobio.2017.07.001

Ralph, M. A., Jefferies, E., Patterson, K., & Rogers, T. T. (2017). The neural and computational bases of semantic cognition. *Nature Reviews. Neuroscience, 18*(1), 42–55. https://doi.org/10.1038/nrn.2016.150

Rolls, E. T., Huang, C. C., Lin, C. P., Feng, J., & Joliot, M. (2020). Automated anatomical labelling atlas 3. *Neuroimage, 206*, 116189. https://doi.org/10.1016/j.neuroimage.2019.116189

Ross, K., & Wertz, R. (2003). Quality of life with and without aphasia. *Aphasiology, 17*(4), 355–364. https://doi.org/10.1080/02687030244000716

Sarubbo, S., Tate, M., De Benedictis, A., Merler, S., Moritz-Gasser, S., Herbet, G., et al. (2020). A normalized dataset of 1821 cortical and subcortical functional responses collected during direct electrical stimulation in patients undergoing awake brain surgery. *Data Brief, 28*, 104892. https://doi.org/10.1016/j.dib.2019.104892

Saur, D., Kreher, B. W., Schnell, S., Kummerer, D., Kellmeyer, P., Vry, M. S., … Weiller, C. (2008). Ventral and dorsal pathways for language. *Proceedings of the National Academy of Sciences, 105*(46), 18035–18040. https://doi.org/10.1073/pnas.0805234105

Saur, D., Schelter, B., Schnell, S., Kratochvil, D., Kupper, H., Kellmeyer, P., … Weiller, C. (2010). Combining functional and anatomical connectivity reveals brain networks for auditory language comprehension. *Neuroimage, 49*(4), 3187–3197. https://doi.org/10.1016/j.neuroimage.2009.11.009

Schomers, M. R., Garagnani, M., & Pulvermuller, F. (2017). Neurocomputational consequences of evolutionary connectivity changes in perisylvian language cortex. *The Journal of Neuroscience: the Official Journal of the Society for Neuroscience, 37*(11), 3045–3055. https://doi.org/10.1523/JNEUROSCI.2693-16.2017

Schwarzer, V., Bahrend, I., Rosenstock, T., Dreyer, F. R., Vajkoczy, P., & Picht, T. (2018). Aphasia and cognitive impairment decrease the reliability of rnTMS language mapping. *Acta Neurochirurgica (Wien), 160*(2), 343–356. https://doi.org/10.1007/s00701-017-3397-4

Smith, R. E., Tournier, J. D., Calamante, F., & Connelly, A. (2012). Anatomically-constrained tractography: Improved diffusion MRI streamlines tractography through effective use of anatomical information. *Neuroimage, 62*(3), 1924–1938. https://doi.org/10.1016/j.neuroimage.2012.06.005

Stensjoen, A. L., Berntsen, E. M., Jakola, A. S., & Solheim, O. (2018). When did the glioblastoma start growing, and how much time can be gained from surgical resection? A model based on the pattern of glioblastoma growth in vivo. *Clinical Neurology and Neurosurgery, 170*, 38–42. https://doi.org/10.1016/j.clineuro.2018.04.028

Stockert, A., Wawrzyniak, M., Klingbeil, J., Wrede, K., Kummerer, D., Hartwigsen, G., … Saur, D. (2020). Dynamics of language reorganization after left temporo-parietal and frontal stroke. *Brain: a Journal of Neurology, 143*(3), 844–861. https://doi.org/10.1093/brain/awaa023

Tate, M. C., Herbet, G., Moritz-Gasser, S., Tate, J. E., & Duffau, H. (2014). Probabilistic map of critical functional regions of the human cerebral cortex: Broca's area revisited. *Brain: a Journal of Neurology, 137*(Pt 10), 2773–2782. https://doi.org/10.1093/brain/awu168

Tuncer, M. S., Salvati, L. F., Grittner, U., Hardt, J., Schilling, R., Bahrend, I., … Picht, T. (2021). Towards a tractography-based risk stratification model for language area associated gliomas. *Neuroimage Clinical, 29*, 102541. https://doi.org/10.1016/j.nicl.2020.102541

Yuan, B., Zhang, N., Yan, J., Cheng, J., Lu, J., & Wu, J. (2020). Tumor grade-related language and control network reorganization in patients with left cerebral glioma. *Cortex, 129*, 141–157. https://doi.org/10.1016/j.cortex.2020.04.015

Yushkevich, P. A., Piven, J., Hazlett, H. C., Smith, R. G., Ho, S., Gee, J. C., et al. (2006). User-guided 3D active contour segmentation of anatomical structures: Significantly improved efficiency and reliability. *Neuroimage, 31*(3), 1116–1128. https://doi.org/10.1016/j.neuroimage.2006.01.015

Zhang, S., & Arfanakis, K. (2018). Evaluation of standardized and study-specific diffusion tensor imaging templates of the adult human brain: Template characteristics, spatial normalization accuracy, and detection of small inter-group FA differences. *Neuroimage, 172*, 40–50. https://doi.org/10.1016/j.neuroimage.2018.01.046